Divergence control of relativistic harmonics by an optically shaped plasma surface

Jian Gao,[1,2] Boyuan Li,[1,2] Feng Liu,[1,2,*] Zi-Yu Chen,[3,4,†] Min Chen,[1,2] Xulei Ge,[1,2] Xiaohui Yuan,[1,2] Liming Chen,[1,2] Zhengming Sheng,[1,2,5,6,7] and Jie Zhang[1,2]

[1]*Key Laboratory for Laser Plasmas (Ministry of Education) and School of Physics and Astronomy, Shanghai Jiao Tong University, Shanghai 200240, China*

[2]*Collaborative Innovation Center of IFSA (CICIFSA), Shanghai Jiao Tong University, Shanghai 200240, China*

[3]*National Key Laboratory of Shock Wave and Detonation Physics, Institute of Fluid Physics, China Academy of Engineering Physics, Mianyang 621999, China*

[4]*Key Laboratory of High Energy Density Physics and Technology (Ministry of Education), College of Physics, Sichuan University, Chengdu 610064, China*

[5]*SUPA, Department of Physics, University of Strathclyde, Glasgow G4 0NG, United Kingdom*

[6]*Cockcroft Institute, Sci-Tech Daresbury, Cheshire WA4 4AD, United Kingdom*

[7]*Tsung-Dao Lee Institute, Shanghai Jiao Tong University, Shanghai 200240, China*

(Received 7 September 2019; revised manuscript received 17 January 2020; accepted 31 January 2020; published 2 March 2020)

The unique spatial and temporal properties of relativistic high harmonics generated from a laser-driven plasma surface allow them to be coherently focused to an extremely high intensity reaching the Schwinger limit. The ultimately achievable intensity is limited by the harmonic wavefront distortions during the interactions. Here we demonstrate experimentally that the harmonic divergence can be controlled by an optically shaped plasma surface with a prepulse that has the same spatial and temporal distribution as the main laser pulse. Simulations are also performed to explain the experimental observation, and we find that the harmonic wavefront curvature from a dented surface can be precompensated by a convex plasma. Our work suggests an active approach to control the harmonic divergence and wavefront by an optically shaped target. This can be critical for further high harmonics applications.

DOI: 10.1103/PhysRevE.101.033202

I. INTRODUCTION

High-order harmonic generation (HHG) through the interactions of intense laser pulses with overdense plasma surfaces is a promising energetic coherent extreme ultraviolet (XUV) source. HHG from plasma surfaces is explained by three main mechanisms: coherent wake emission (CWE) [1], relativistically oscillating mirror (ROM) [2–4], and coherent synchrotron emission [5,6]. An alternative theory of relativistic electronic spring has also been proposed [7,8]. Previous experiments demonstrated that HHG from a plasma surface driven by a petawatt laser can generate coherent x-ray pulses at wavelengths in the "water-window" region [9]. In the time domain, the radiation is confined in a very short temporal window in each optical cycle, leading to the generation of an attosecond pulse train [10]. Even single isolated attosecond pulse could be obtained by various gating techniques, including amplitude gating by few-cycle laser pulses [11,12], noncollinear polarization gating [13], and the attosecond lighthouse [14,15]. Simulations indicate that the polarization of HHG is also fully controllable by the laser and plasma parameters [3,16,17]. These exciting advances pave the way for the wide applications of such a coherent XUV source, such as plasma and magnetic materials diagnostics [18–20], high-resolution imaging [21,22], and seeding free-electron lasers [23].

It is predicted that the harmonics could be coherently focused to an unprecedentedly high intensity even reaching the Schwinger limit to study the peculiar nonlinear quantum electrodynamics effects [24–26]. However, focusing of the harmonics is still challenging. A plasma mirror has been experimentally demonstrated to boost the laser intensity [27]. It is almost impossible to make such a mirror with micrometer-scale size. A curved plasma surface created by the laser radiation pressure is proposed to combine the generation and focusing of harmonics [26]. This scheme works only for a petawatt laser. If the harmonics are focused in the far field by optics, the ultimately focused intensity is limited by effects such as intrinsic phase [28,29] and target surface denting [30,31] during the interactions, which lead the harmonic wavefront to deviate from an ideal plane or spherical wavefront. The intrinsic phase is due to the laser intensity-dependent electron dynamics, which is the dominant effect for CWE harmonics. And the surface denting arises from the strong laser radiation pressure, which is the dominant effect for ROM harmonics. Major efforts have been made to mitigate the harmonic wavefront curvature. Moving the target away from the laser best focus can only partially compensate for harmonic wavefront curvature of intrinsic phase [28] and target surface denting [32], because the phase imposed to the harmonics by the

*liuf001@sjtu.edu.cn
†ziyuch@scu.edu.cn

 ©2020 American Physical Society

intrinsic phase and the surface denting are also Gaussian in shape for a Gaussian laser spot. Moreover, a much higher laser power is needed to achieve the same intensity. Another route is to use targets with specially designed shapes to compensate for the harmonic wavefront curvature induced by target denting effect. A shaped target with a convex surface has also been proposed in simulations [33]. It is difficult to fabricate and precisely align the target to exactly match the focused laser intensity distribution.

In this paper, we demonstrate a practical implementation to produce a suitable curved target shape. The target surface shaping is optically achieved by a prepulse that has the same spatial and temporal distribution as the main laser pulse. In this way, the preplasma shape naturally matches the main pulse intensity distribution. Experiments are carried out to confirm the generation of such a curved target shape by the observation of significantly enlarged harmonic divergence at the laser intensity level of 10^{19} W/cm^2, which is well supported by two-dimensional particle-in-cell (PIC) simulations. At much higher intensity, simulation results suggest that this method can effectively compensate for the target denting and actively control the harmonic divergence.

II. EXPERIMENTAL DETAILS

The experiments are carried out with the 200 TW Ti:sapphire laser system (800 nm, 10 Hz) at the Laboratory for Laser Plasmas of Shanghai Jiao Tong University. The amplified spontaneous emission contrast of the laser is improved to be better than 10^{-11} at 10 ps prior to the main peak by combining a single plasma mirror system [34] and a cross-polarized wave generation technique [35]. Due to the transmission of the plasma mirror system, a p-polarized laser beam with an on-target energy of $E = 1$ J is used in the experiments. The laser beam with a pulse duration of $\tau = 29$ fs (full width at half maximum, FWHM) is focused onto polished fused silica plates by an $f/4$ off-axis parabola (OAP) mirror with a focal spot size of 6 μm (FWHM). The peak intensity of the pulse on the target is $I = 3 \times 10^{19}$ W/cm^2 (normalized vector potential $a_0 = 3.7$). The high-order harmonic radiations are measured with a flat-field spectrometer.

Figure 1 schematically shows the experimental setup. As shown in Fig. 1(b), the convex plasma surface is produced by prepulse P1, which is introduced by an ultrafast pulse shaper (Dazzler, Fastlite) in the laser front end. The delay and energy of P1 with respect to the main pulse can be tuned by the pulse shaper. P1 goes ahead of the main pulse through the whole laser amplifier chain, so that they have the same spatial and temporal characteristics. Owing to the same focal spot size with lower intensity, the density profile of the preplasma generated by P1 varies within the focal spot of the main pulse. A convex plasma surface is optically created when the main pulse arrives. The harmonic generation efficiency is optimized by P1 with $a_0 = 0.4$ and delay of 2 ps. The plasma density scale length $L = 0.17\lambda$ is estimated using 1D PIC simulations [36].

As shown in Fig. 2(a), relativistic ROM harmonics with maximum order $H_{\max} = 46$ are observed at a laser specular direction when the laser incidence angle is 40°. The spectrum decays as a power law with $I \propto H^{-8/3}$ (H is harmonic order),

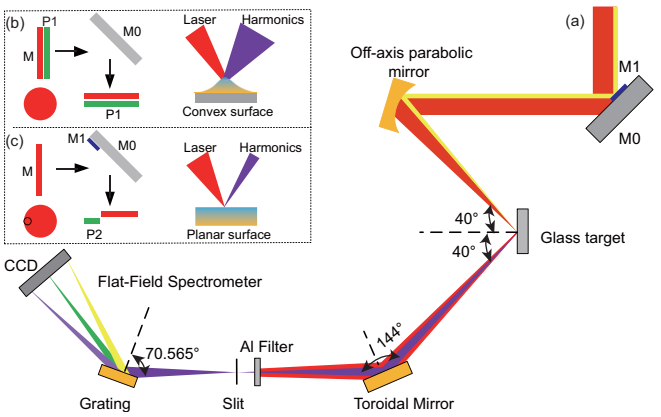

FIG. 1. (a) The schematic illustration of the experimental setup. (b) A convex plasma surface is generated by prepulse P1 introduced by an ultrashort pulse shaper. (c) A planar plasma surface is generated by prepulse P2 introduced by a small mirror M1. M is the main pulse.

which is in accordance with BGP theory [4]. The harmonic radiations are usually observed to be highly collimated on the reflected laser axis with a divergence of tens of mrads [30,37]. However, in our experiments, the harmonic divergence is observed to be significantly enlarged by the convex plasma surface, which is verified by the fact that intense harmonics are also measured far from the laser specular axis. The acceptance angle of the spectrometer is only 40 mrad, and the target chamber window used to install the spectrometer is limited. In order to demonstrate the much larger harmonic divergence, the target is rotated to let the spectrometer out of the reflected laser cone. Even though the harmonic generation efficiency is affected by the changed laser incidence angle [37], strong harmonics are also obtained off the reflected laser axis as shown in Fig. 2(b), when the laser incidence angle is 20° and the detection angle is 60°. Differently from the scaling law of $I \propto H^{-8/3}$, the spectrum decays more slowly with a nearly flat roll-off tendency.

In order to compare the harmonic divergence respectively generated by a convex and a planar plasma surface, prepulse P2 is introduced by another way to generate a homogeneous preplasma within the main pulse focal spot [38]. As shown in Fig. 1(c), P2 is obtained by a 2-inch reflection mirror M1, which is placed in the front of a large mirror M0 (200 mm × 140 mm) to reflect a small part of the main pulse. Changing the reflective area of M1, the intensity of P2 can be adjusted. The delay of P2 can be precisely tuned by the distance between M1 and M0. P2 is controlled to be ahead of the main pulse with $a_0 = 0.2$ and delay of 3 ps to generate the same $L = 0.17\lambda$ for efficient harmonic generation. Since the beam size of P2 is much smaller than the main pulse, focused by the same OAP, the focal spot of P2 (53 μm × 14 μm, FWHM) is much larger than the main pulse (6 μm, FWHM). The plasma surface for the main pulse can be regarded as a planar surface when it arrives.

Figures 3(a) and 3(b) show the two raw spectral images with P1 and P2, respectively, at a laser incidence angle of 40° and detection angle of 40°. The harmonic divergence is significantly enlarged by the convex plasma surface. The

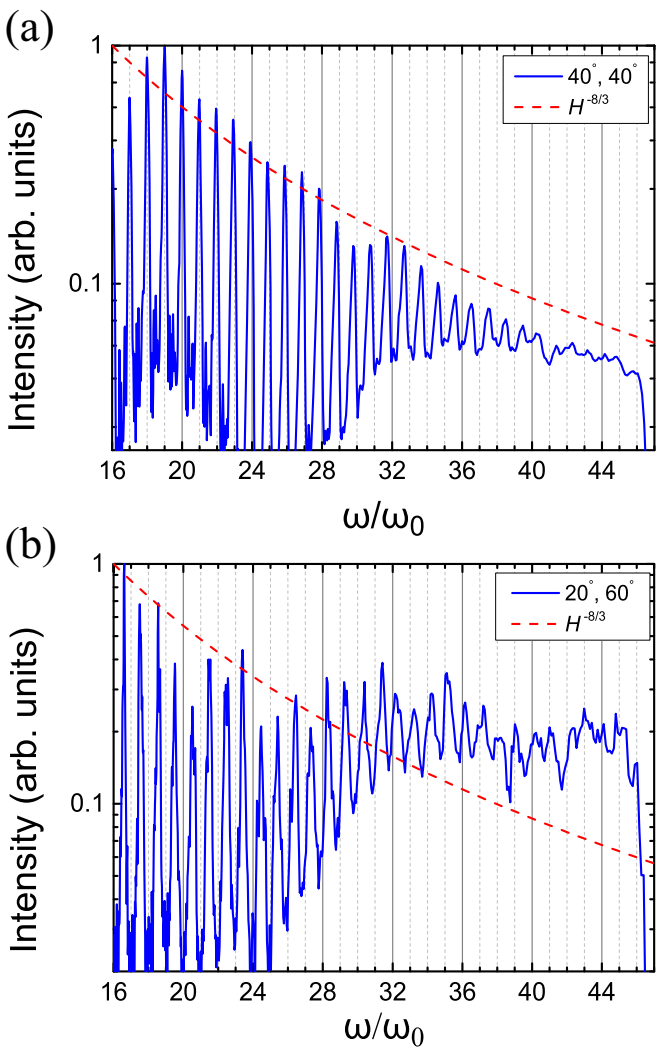

FIG. 2. The spectra of high-order harmonics obtained with prepulse P1 in experiments: (a) harmonics are measured at specular direction when the laser incidence angle is 40°; (b) harmonics are measured off the reflected laser axis at 60° to the target normal direction when the laser incidence angle is 20°. The red dashed lines mark the scaling $I \propto H^{-8/3}$.

harmonic divergences of the 26th order from the two cases are compared in Fig. 3(c). The harmonic divergence with P2 is fitted with a Gaussian profile to be 22.5 mrad (FWHM). On the other hand, the harmonic angular distribution with P1 is nearly flat. The divergences (FWHM) measured for harmonic orders from 21st to 31st in the case of a planar surface are presented in Fig. 3(d). It can be clearly seen that the divergence decreases with the harmonic order, which is in accordance with the diffraction-limited curve $\theta_H = \theta_{\text{laser}}/H$. The experimental results show that at our laser intensity of $I = 3 \times 10^{19}$ W/cm^2, the target surface denting effect is not significant.

The potential different L between P1 and P2 partially influences the harmonic divergence [39]. However, the divergence varies within the reflected laser cone when only L is changed [30,32,38]. The harmonic divergence much larger than the

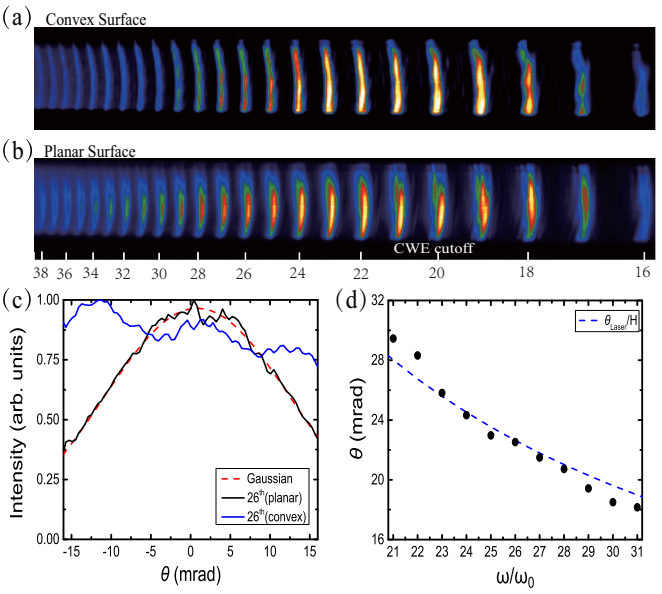

FIG. 3. The raw spectral images of harmonic radiations from a convex plasma surface (a) and a plane plasma surface (b). (c) The angular distributions of the 26th-order harmonic in the two cases. (d) The measured divergences (FWHM) of harmonics from 21st to 31st orders by a planar surface. The blue dashed line indicates the diffraction-limited divergence.

reflected laser cone should be mainly attributed to the convex plasma surface.

III. 2D PARTICLE-IN-CELL SIMULATIONS

To further support the experimental results and show the plasma surface shaping effect on HHG more clearly, we carried out 2D particle-in-cell (PIC) simulations using the VLPL code (Virtual Laser Plasma Laboratory) [40]. The key parameters for the laser and plasmas are close to those in the experiments. A p-polarized laser pulse is in the x-y plane with $\lambda_0 = 800$ nm and $a_0 = 3.7$. The incident angle is taken to be $\alpha = 20°$, which is the same as Fig. 2(b). The laser pulse profile is Gaussian both temporally and spatially with a pulse duration of $7T_0$ (FWHM, T_0 is laser period) and a focal spot size of $3\lambda_0$ (FWHM). The fully ionized plasma target is composed of a uniform slab with density $n_{e0} = 100n_c$ and a preplasma with an exponential density gradient profile $n_e(x) = n_{e0} \exp[(x - x_0)/L_s(y)]$ in the x direction, where $x_0 = 45\lambda_0$ is the position of the plasma-slab front surface. To simulate the shaped plasma surface effects in the experiments, we consider two transverse preplasmas profiles, i.e., with a Gaussian-shaped $L_s(y) = L \exp(-y^2/4w_0^2)$ ($w_0 = 3\lambda_0$) and uniform density distribution $L_s(y) = L$. L is $0.17\lambda_0$ in both profiles. The resultant electron density distributions are shown in Figs. 4(a) and 4(b), respectively. The ions are assumed to be immobile during the interactions. The size of the simulation box is $55\lambda_0 \times 60\lambda_0$. The grid step is $\lambda_0/200 \times \lambda_0/200$, and the time step is $0.0035T_0$.

In order to save computation resources and simulation time, we shorten the focal spot size to $3\lambda_0$ and the pulse duration to $7T_0$. The surface denting is not sensitive to laser

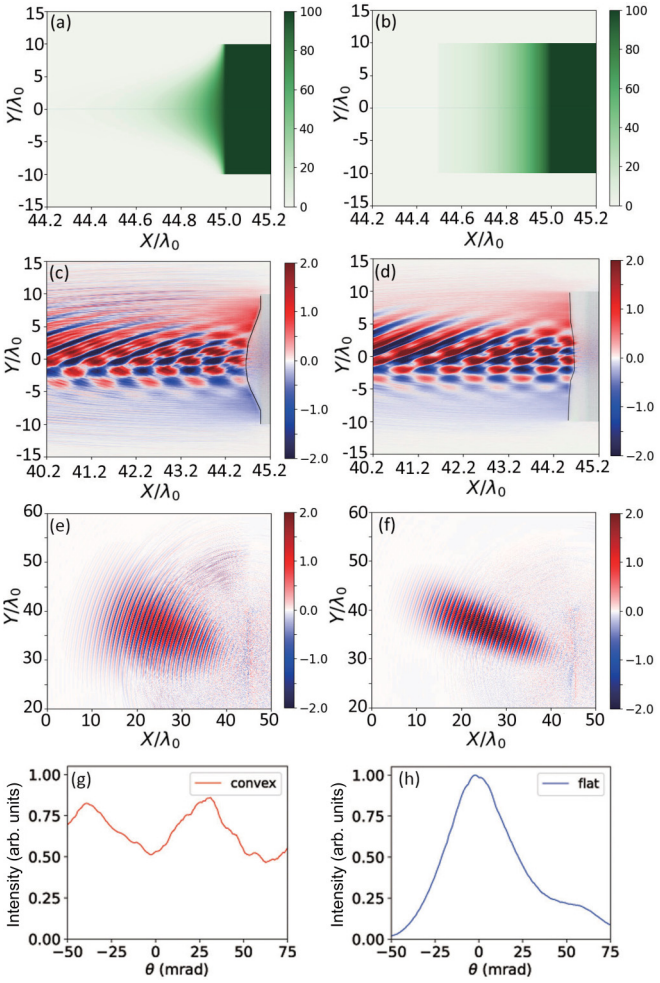

FIG. 4. The plasma density maps of targets (a), (b), snapshots of the magnetic field component B_z during the interactions at $t = 36T_0$ (c), (d), spatial distribution of the reflected magnetic field B_z after the interactions at $t = 48T_0$ (e), (f) and the divergence of harmonics from fifth to ninth orders (g), (h) for transversely Gaussian-shaped (left column) and uniform density distribution (right column). The laser is incident from the lower left corner and reflected towards the upper left.

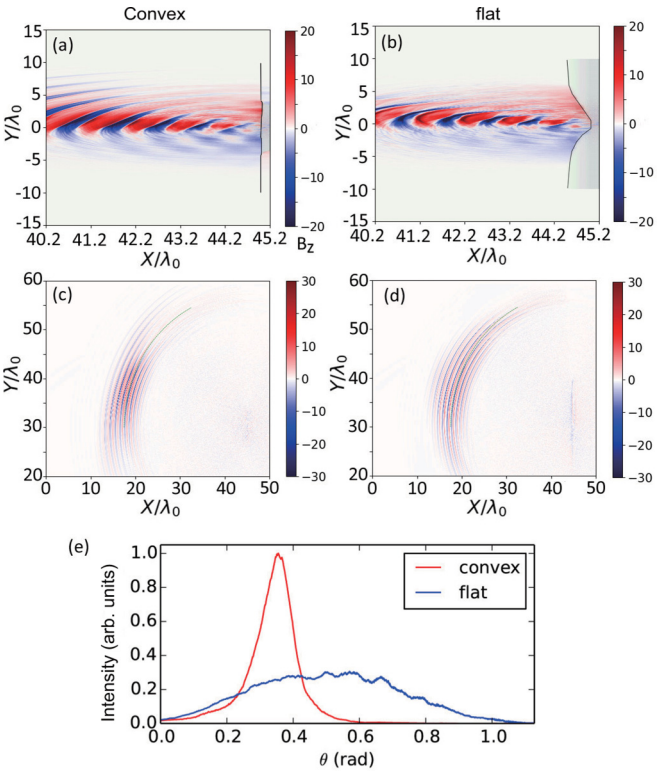

FIG. 5. Simulation results at a higher laser intensity ($a_0 = 37$). Snapshots of the magnetic field component B_z during the interactions at $t = 24T_0$ (a), (b), and spatial distribution of the reflected magnetic field B_z after the interactions at $t = 48T_0$ (c), (d) for transversely Gaussian-shaped (left column) and uniform density distribution (right column). (e) Normalized intensities of the reflected fields along their wavefronts (the dotted green lines) in panels (c) and (d).

pulse duration, but it is mainly determined by the laser intensity [30,39]. In addition, the transverse profile of the convex plasma in y direction is Gaussian with $w_0 = 3\lambda_0$, which is the same as the laser focal spot size in simulations. Figures 4(c) and 4(d) present two snapshots of the magnetic field component B_z as well as the plasma density with $n_e > 1$ (i.e., above the critical density) during the laser-plasma interactions. It can be seen clearly from Fig. 4(c) that the wavefront of the reflected field is significantly curved because of reflection from the convex plasma surface. This should largely affect the divergence of the reflected pulse in the far field, although the convex preplasma has a small thickness of only a few hundred nanometers (notice the different scale in the x and y axes). In contrast, the reflected field from the transversely flat plasma mirror exhibits a straight wavefront pattern, as shown in Fig. 4(d). The spatial distribution of the reflected field after the interaction is shown in Figs. 4(e) and 4(f). The divergence of the reflected pulse from the convex plasma is considerably larger than that from the transversely flat target. Due to the limited resolution of the 2D PIC simulations, harmonics up to about 10th order could be numerically resolved. In order to compare with experiments, the simulated divergence of harmonics from fifth to ninth orders is plotted in Figs. 4(g) and 4(h). The divergence distribution for the convex plasma surface is nearly flat. In contrast, the harmonics from the planar plasma surface have a much smaller divergence of 44 mrad. These results are in accordance with experiments.

The above experimental and simulation results are carried out at a relatively low laser intensity, where the plasma surface denting effect is not significant [see Fig. 4(d)]. The resultant harmonic divergence from a convex plasma surface is thus larger than that from a flat surface. Under ultraintense laser radiation with tight focusing, however, the target surface will be dented. The above experimental and simulation results suggest that the initially convex plasma surface may be useful to compensate the surface denting and control the harmonic divergence. To demonstrate this with an acceptable computation time, we increase the laser intensity by a factor of hundred ($a_0 = 37$), decrease the spot size to $1\lambda_0$, and shorten the pulse duration to $2T_0$. The other simulation parameters remain unchanged. The extra simulations with mobile ions are

also performed, which show the same results with immobile ions. From Figs. 5(a) and 5(b), it can be seen that the target shape during the interaction has been significantly modified by the light pressure. The plasma surface is nearly flat for an initially convex plasma surface while largely dented for an initially flat surface. Figures 5(c) and 5(d) show the reflected field distribution in the far field. The severely dented plasma surface deflects the reflected fields into a large angular range [see Fig. 5(d)]. In comparison, the beam divergence from the initially convex plasmas is markedly reduced along with a much higher intensity [see red line in Fig. 5(e)]. Our simulation results shown above well reproduce the main experimental observations and demonstrate the great potential of an optically shaped plasma surface to control the HHG divergence.

IV. CONCLUSIONS

In conclusion, we have demonstrated experimentally and numerically that the harmonic divergence can be controlled by an optically created convex plasma surface. Under our conditions with the laser intensity about 10^{19} W/cm^2, the divergence of harmonics from the convex plasma surface is found to be much larger than that from a planar plasma surface. However, when the laser intensity goes much higher such as 10^{21} W/cm^2, according to our simulations, due to the optically shaped surface, the harmonics are radiated into a significantly smaller angle along with a much higher intensity. Our results suggest a practical approach to control the harmonic divergence by tailoring the curvature of the shaped convex surface. The harmonic wavefront curvature due to the target denting effect could be precompensated by a convex surface with suitable shape. This could be critical to focus the relativistic high harmonics to achieve unprecedented intensities in the future.

ACKNOWLEDGMENTS

The research has received support from National Natural Science Foundation of China (Grants No. 11721091, 11775144, 11705185, and 11905129), Natural Science Foundation of Shanghai (Grant No. 18ZR1419200), Science Challenge Project (Grant No. TZ2018005), CAEP Presidential Fund (YZJJLX2017002), and a project funded by the China Postdoctoral Science Foundation (Grant No. 2017M621443). Simulations were performed on the PI Supercomputer at SJTU.

[1] F. Quéré *et al.*, Phys. Rev. Lett. **96**, 125004 (2006).
[2] S. V. Bulanov *et al.*, Phys. Plasmas **1**, 745 (1994).
[3] R. Lichters *et al.*, Phys. Plasmas **3**, 3425 (1996).
[4] T. Baeva *et al.*, Phys. Rev. E **74**, 046404 (2006).
[5] D. an der Brügge *et al.*, Plasmas **17**, 033110 (2010).
[6] B. Dromey *et al.*, Nat. Phys. **8**, 804 (2012).
[7] A. Gonoskov *et al.*, Phys. Rev. E **84**, 046403 (2011).
[8] A. Gonoskov *et al.*, Phys. Plasmas **25**, 013108 (2018).
[9] B. Dromey *et al.*, Nat. Phys. **2**, 456 (2006).
[10] Y. Nomura *et al.*, Nat. Phys. **5**, 124 (2009).
[11] P. Heissler *et al.*, Phys. Rev. Lett. **108**, 235003 (2012).
[12] D. Kormin *et al.*, Nat. Commun. **9**, 4992 (2018).
[13] M. Yeung *et al.*, Phys. Rev. Lett. **115**, 193903 (2015).
[14] H. Vincenti *et al.*, Phys. Rev. Lett. **108**, 113904 (2012).
[15] J. A. Wheeler *et al.*, Nat. Photonics **6**, 829 (2012).
[16] Z.-Y. Chen *et al.*, Nat. Commun. **7**, 12515 (2016).
[17] Z.-Y. Chen *et al.*, Opt. Express **26**, 4572 (2018).
[18] M. Drescher *et al.*, Nature (London) **419**, 803 (2002).
[19] A. Malvache *et al.*, Phys. Rev. E **87**, 035101 (2013).
[20] C. von Korff Schmising *et al.*, Phys. Rev. Lett. **112**, 217203 (2014).
[21] H. N. Chapman *et al.*, Nat. Phys. **2**, 839 (2006).
[22] A. Ravasio *et al.*, Phys. Rev. Lett. **103**, 028104 (2009).
[23] B. H. Shaw *et al.*, J. Appl. Phys. **114**, 043106 (2013).
[24] S. Gordienko *et al.*, Phys. Rev. Lett. **94**, 103903 (2005).
[25] F. Karbstein *et al.*, Phys. Rev. Lett. **123**, 091802 (2019).
[26] H. Vincenti, Phys. Rev. Lett. **123**, 105001 (2019).
[27] M. Nakatsutsumi *et al.*, Opt. Lett. **35**, 2314 (2010).
[28] F. Quéré *et al.*, Phys. Rev. Lett. **100**, 095004 (2008).
[29] M. Yeung *et al.*, Phys. Rev. Lett. **110**, 165002 (2013).
[30] B. Dromey *et al.*, Nat. Phys. **5**, 146 (2009).
[31] M. Behmke *et al.*, Phys. Rev. Lett. **106**, 185002 (2011).
[32] H. Vincenti *et al.*, Nat. Commun. **5**, 3403 (2014).
[33] R. Hörlein *et al.*, Eur. Phys. J. D **55**, 475 (2009).
[34] X. L. Ge *et al.*, Chin. Opt. Lett. **16**, 103202 (2018).
[35] A. Jullien *et al.*, Opt. Lett. **30**, 920 (2005).
[36] J. Gao *et al.*, Phys. Plasmas **26**, 103102 (2019).
[37] C. Thaury *et al.*, J. Phys. B: At. Mol. Opt. Phys. **43**, 213001 (2010).
[38] S. Kahaly *et al.*, Phys. Rev. Lett. **110**, 175001 (2013).
[39] A. Leblanc *et al.*, Phys. Rev. Lett. **119**, 155001 (2017).
[40] A. Pukhov, J. Plasma Phys. **61**, 425 (1999).